

NUMERICAL INVESTIGATION OF CAPILLARY BARRIER PERFORMANCE WITH TRANSPORT LAYER

G. H. Yunusa^{1*}, A. Kassim¹, Z. Abu Talib²

Department of Geotechnics and Transportation, Faculty of Civil Engineering
Universiti Teknologi Malaysia

Corresponding Author email: azmankassim@utm.my

Keywords: Capillary barrier, transport layer, seepage analysis, diversion length, breakthrough time

Abstract: A capillary barrier is a promising alternative measure for controlling rainfall infiltration in unsaturated residual soil slopes. Although, capillary barriers have been successfully applied to avert rainfall infiltration in dry and semi-dry climates, its application in humid climates with high precipitation rate is still unsatisfactory. Therefore, this paper evaluates the performance of modified capillary barrier with transport layer under humid climates. The capillary barrier was simulated with Grade V and Grade VI soil and the transport layer was made with gravel material. The complete slope model was subjected to a 24-hour rainfall intensity of 14.6 mm/hr using saturated/unsaturated seepage analysis software (Seep/W). The results show that the diversion length and breakthrough time were greatly improved in the modified capillary barrier with transport layer than the conventional capillary barrier system. Therefore, the inclusion of transport layer in a residual soil capillary barrier improved its performance.

I. INTRODUCTION

A capillary barrier is a two layered soil system consisting of fine-grained soil layer overlying a coarse-grained soil layer (Ross, 1990; Stormont, 1996). The contrast in particle sizes causes variation in hydraulic properties between the two soil layers and creates a capillary break at interface that impedes downward movement of water into the coarse-grained layer. Capillary barrier can be classified into natural capillary barrier forming from weathering process or engineered (artificial) capillary barrier constructed from selected soil materials (Lu and Godt, 2013).

Rainfall-induced slope failure is a natural disaster usually associated with loss of lives and properties in various parts of the world. The principle of capillary barrier is used as slope stabilization method which prevents this type of failure by averting rainfall infiltration into unsaturated slope (Li et al., 2013; Rahardjo et al., 2012; Tami et al., 2004). The shortcoming of using capillary barrier system for slope stabilization in humid climates with high precipitation rate is breakthrough occurrence which renders the system ineffective. Hence, a transport layer is proposed to extend the application of capillary barrier to humid climates. Therefore, in this study, a saturated/unsaturated commercial finite element software, Seep/w (Geo-Slope International, 2007) was used and performed a numerical analysis for capillary barrier and transport layer.

II. MATERIALS AND METHODS

The materials used in this study are grade V and grade VI soils and gravel. The grade V and grade VI soils are classified as silty gravel of high plasticity (GMH) and sandy silt of very high plasticity (MVS), respectively. The grade VI and grade V are used as fine-grained and coarse-grained layers, respectively. Similarly,

the gravel is classified as uniformly graded gravel (G_{pu}) and is used as transport layer. The particle size distribution (PSD) curve, soil water characteristic curve (SWCC) and hydraulic conductivity function (HCF) of these materials are shown in Figs. 1, 2 and 3, respectively.

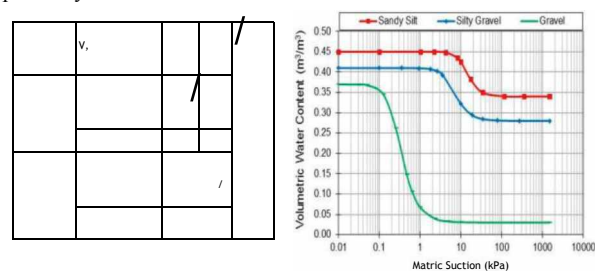


Figure 1. PSD of the materials Figure 2. SWCC of the materials

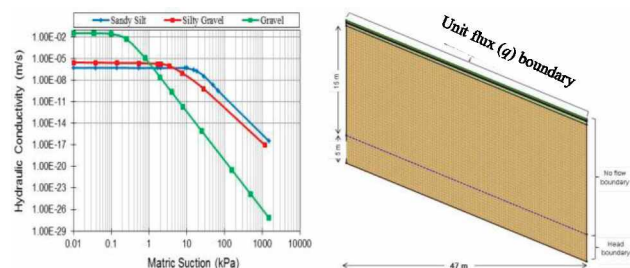


Figure 3. HCF of the materials Figure 4. Numerical slope model

The numerical slope model used in the numerical analysis is shown in Figure 4. The slope is inclined at an angle of 21° with a slope length of 47 m. The finite element mesh of the numerical slope model consists of 6222 nodes and 6060 quadrilateral mesh elements. A Groundwater table was located at 15 m below the ground surface and therefore, head boundaries were applied along the left and right edges below the water table with pressure head equal to the vertical distance from the water table. The left and right edges above the water table were assigned as zero flux boundaries (i.e. $g = 0$). Finally, rainfall intensity is modelled as unit flux (\hat{q}) and is applied as infiltration on the exposed sloping surface.

III. RESULTS AND DISCUSSION

Variation of Pore water pressure in soil System without Transport Layer

The variation of negative pore water pressure at the interface of the two soil layers due to variation of grade VI residual soil layer thickness is presented in Fig. 5. This Figure shows that the breakthrough time increases with increase in thickness of grade VI residual soil layer. This observation indicated that as the thickness of grade VI residual soil layer increases, the time for the infiltrating water to reach the interface will also increase. This implies that

the depth of wetting front increases with increase in grade VI residual soil layer thickness.

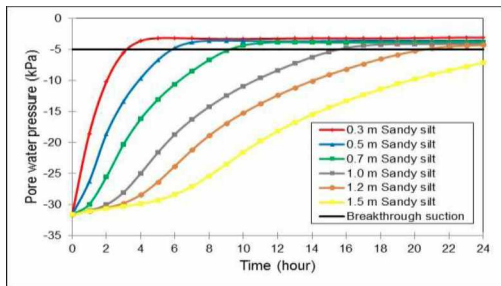


Figure 5. Variations of pore water pressure with time

The variation of negative pore water pressure with distance along the interface at the end of 24-hour rainfall duration is presented in Fig. 6. This Fig. shows that the infiltrating water has reaches the interface of the two soil layers and uniformly reduces the negative pore water pressure below the breakthrough suction of -5.0 kPa (-5.0 kPa was determined as intersection point of hydraulic conductivity curves). The uniform decrease in negative pore water pressure was observed even when the thickness of grade VI residual soil layer was increased to 150 cm. Therefore, the diversion length for these combinations of grade VI residual soil thicknesses is approximately 1.5 m.

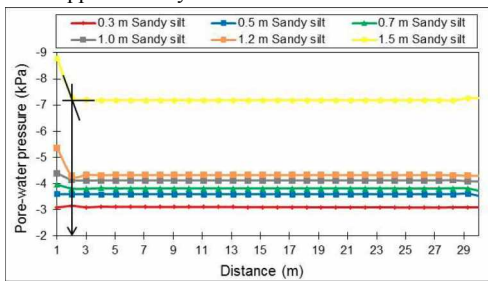


Figure 6. Variations of pore water pressure with distance

Variation of Pore water pressure in soil System with Transport Layer

The variation of pore water pressure with time due to the 24-hour rainfall intensity of 14.6 mm/hr is presented in Fig. 7. The negative pore water pressure is maintained as initial condition (i.e. -32 kPa) for almost 8 hours when a transport layer was inserted at the interface of the two soil layers. Within this time, the infiltrating water was laterally diverted towards the toe of the slope model. After 8 hours the negative pore water pressure decreases to -22 kPa up to the end of rainfall duration. This shows that after 8 hours, the infiltrating water penetrates the gravel layer and diverted through it for the remaining analysis periods. From this observation, it is clear that the variation in the hydraulic conductivity of gravel and grade VI residual soil forms hydraulic impedance that limits downward movement of the infiltrating water. The infiltrating water is retained in the grade VI residual layer and flow laterally above the interface. The diversion length was determined using a tangent method as explained by Aubertin, et al., (2009). Fig. 8 shows the diversion length for the slope model due to 24-hour rainfall pattern. This Fig. shows that the infiltrating water was diverted above the interface of transport layer and grade VI residual soil layer up to 16 m before it eventually infiltrates the grade V residual soil layer.

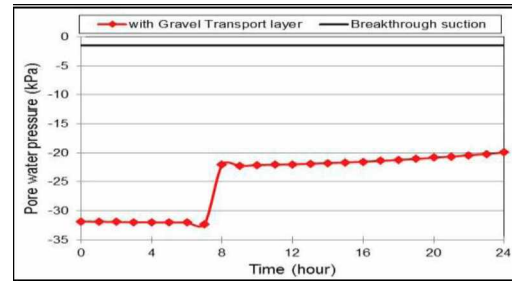


Figure 7. Variations of pore water pressure with time for a system with transport layer

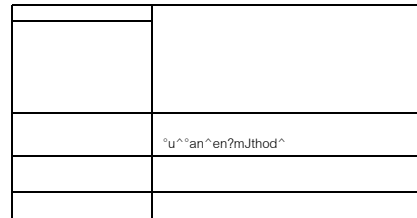


Figure 8. Diversion length for system with transport layer

IV. CONCLUSIONS

Based on the findings from this study, the following conclusions may be drawn:

- (i) The arrangement of grade V and grade VI soil system due to weathering process forms a capillary barrier which impedes downward movement of infiltrating water.
- (ii) Gravel developed high hydraulic impedance which facilitates lateral flow of infiltrating water above the interface.
- (iii) A transport layer significantly improved the breakthrough time and diversion length of a natural capillary barrier constructed from residual soils.

REFERENCES

- [1] Aubertin, M., E. Cifuentes, S. A. Apithy, B. Bussiere, J. Molson, and R. P. Chapuis. 2009. Analyses of water diversion along inclined covers with capillary barrier effects. *Caww'aw Geo'ecAw'caJ JoMrwaJ*. 46(10), 1146-1164.
- [2] Geo-Slope international, 2007. <SEEP/W User's gM/Je ybr e/emew^ seepage awa/yM'M. Geo-6*Jope iw^erwa^owa/ ZM Calgary, Alta.
- [3] Li, J. H., L. Du, R. Chen, and L. M. Zhang. 2013. Numerical investigation of the performance of covers with capillary barrier effects in South China. *CompM^erM aw^ Geo^ecAw^c^*. 48(0), 304-315.
- [4] Lu, N. and J. W. Godt. 2013. *H'/Mope Hy^ro/ogy aw^ .SYaM^Yy*. Cambridge University Press.
- [5] Rahardjo, H., V. A. Santoso, E. C. Leong, Y. S. Ng, and C. J. Hua. 2012. Performance of an Instrumented Slope Covered by a Capillary Barrier System. *JoMrwaJ o/ Geo^ecAw'caJ aw^ Geoeww^rowmew^aJ Ewg^weer^wg*. 138(4), 481-490.
- [6] Ross, B., 1990. The diversion capacity of capillary barriers. *PFa^er Re^oMrce^ Re^earcA*. 26(10), 2625-2629.
- [7] Stormont, J. C., 1996. The effectiveness of two capillary barriers on a 10% slope. *Geo^ecAw'caJ & Geo/og^ca/ Ewg^weer^wg*. 14(4), 243-267.
- [8] Tami, D., H. Rahardjo, E. C. Leong, and D. G. Fredlund. 2004. A Physical Model for Sloping Capillary Barriers. *Geo^ecAw'ca/ Tie^i^wg JoMrwaJ*. 27(2), 347-355